Available online at www.sciencedirect.com
SCIENCE DIRECT®
Journal of the European Ceramic Society 25 (2005) 2003–2007
www.elsevier.com/locate/jeurceramsoc

Synthesis and characterization of monazite-type Sr:$LaPO_4$ prepared through coprecipitation

S. Gallini, J.R. Jurado, M.T. Colomer *

Instituto de Cerámica y Vidrio, CSIC, Campus de Cantoblanco (UAM), 28049 Madrid, Spain

Available online 30 March 2005

Abstract

A coprecipitation method was used to obtain $La_{(1-x)}Sr_xPO_4$ ($x = 0$, 0.025, 0.05, 0.10) powders from the following precursors: $La(NO_3)_3{\cdot}6H_2O$, $Sr(NO_3)_2$ and $(NH_4)_2HPO_4$. Several analysis methods were applied in order to study powder morphology and particle size, thermal evolution and sintering behavior of green compacts. Although the electrical properties of these materials have been studied, their synthesis and characterization are still open and barely studied issues in the literature. XRD patterns of the as-prepared powders display the typical peaks of phase-pure $LaPO_4$ (monazite, standard PDF 32-0493 pattern), and also for all the studied compositions and calcination temperatures. TGA data exhibit a 20% weight loss, up to 250 °C, that can be attributed to the residual water and the decomposition of NH_4NO_3, a byproduct of the coprecipitation. The presence of NH_4NO_3 was also confirmed by DTA data and Nitrogen content analysis of the powders. It was found that strontium additions enhanced densification. After sintering at 1200 °C for 4 h in air, the materials showed relative densities higher than 99% of the theoretical density. None of the analyses performed showed any significant difference between Sr-doped and the undoped powders, except for the dilatometric studies. No second phases are observed in the sintered materials. The stability of the sintered samples was studied in high water–vapor partial pressure. The samples were stable in the essayed conditions (pH_2O 2.7–11.5 atm, 120–170 °C for 48 h) as confirmed by XRD, weight measurements and scanning electron microscopy coupled to energy dispersive X-ray spectroscopic analysis (SEM–EDS).

Keywords: Powders-chemical preparation; Calcination; Fuel cells; Phosphates

1. Introduction

Rare-earth phosphates present interesting and unusual physical properties (optical, magnetic, etc.). In recent years, lanthanum phosphate has become a new subject of research for its possible application as a high temperature protonic conductor (HTPC).[1,2] This characteristic is very important for several devices, like fuel cells, hydrogen separators and hydrogen sensors.[3] $LaPO_4$ is a candidate for the transport of protons at high temperatures because it is very stable in atmospheres rich in water vapor and, at the same time, the size of the La^{3+} ion and the open crystalline structure facilitate proton mobility. For this reason, it might find use in solid oxide fuel cells (SOFC) as an electrolyte. However, one of the main problems which has been revealed in a former study is the possible presence of a second phase, probably $Sr_3La(PO_4)_3$, for doping percentages higher than 5 mol% after sintering.[4] It is well known that impurities are an obstacle for the proton mobility and are the cause of a loss of conductivity. At the same time, it is important that the preparation is fast and cheap and gives dense and gas-tight materials (>93% of the theoretical density).[5] Furthermore, the synthesis and characterization of this material are still open issues in the literature.

The aim of this work is to obtain a protocol for the synthesis of pure $La_{(1-x)}Sr_xPO_4$ materials. Several analysis methods were applied in order to study the powder morphology and particle size, the thermal evolution and the sintering behavior of the green compacts. The preparation method was the coprecipitation of $La(NO_3)_3{\cdot}6H_2O$, $Sr(NO_3)_2$ and $(NH_4)_2HPO_4$ as precursors at room temperature and the

* Corresponding author. Tel.: +34 917355858; fax: +34 917355843.
E-mail address: tcolomer@icv.csic.es (M.T. Colomer).

0955-2219/$ – see front matter © 2005 Elsevier Ltd. All rights reserved.
doi:10.1016/j.jeurceramsoc.2005.03.004

studied compositions were $La_{(1-x)}Sr_xPO_4$ (where $x = 0$, 0.025, 0.05 and 0.10).

2. Experimental

2.1. Powder synthesis

As mentioned above, powders of nominal composition $La_{(1-x)}Sr_xPO_4$ ($x = 0$, 0.025, 0.05 and 0.10) were prepared using the following precursors: $La(NO_3)_3{\cdot}6H_2O$, $Sr(NO_3)_2$ and $(NH_4)_2HPO_4$. All the chemicals were purchased from Panreac Química S.A., Barcelona, Spain. Precursors solutions (0.2 M) were prepared and standardized through coupled inductively plasma-atomic emission spectrometry (ICP-AES) (Yobin-Ibon JY-38VHR). The $(NH_4)_2HPO_4$ solution was mixed drop by drop, speed 5 ml/min, at room temperature with the solution of the lanthanum and strontium nitrates (constantly stirred), in order to obtain $La_{(1-x)}Sr_xPO_4$ gels (final pH = 1). The precipitation takes place spontaneously and instantaneously; the gel is then separated by the liquid by means of a 0.8 μm filter (Millipore Inc., USA). The choice of the filter size was made after measuring the agglomerate size by laser diffraction (see Section 3).

After filtering, the product was dried at 105 °C for 80 h. The dried material was crushed using an agate mortar and sieved through a 100 μm sieve. The powders were calcined at three different temperatures (200, 400 and 800 °C) in air, for 12 h at a heating rate of 2 °C/min. The next step was attrition milling in ethanol for 3 h using tetragonal zirconia balls (3Y-TZP, Tosoh). Finally, the powders were sieved again through 100 μm sieve.

2.2. Characterization of powders and sintered materials

Differential thermal analysis–thermogravimetry (DTA–TG) of the as-prepared powders was performed in air with a NETZSCH STA-409 thermoanalyzer, in the range 20–1350 °C and a heating rate of 3 °C/min, calcined alumina was used as reference material. NH_4NO_3 commercial powder (Panreac Química S.A., Barcelona, Spain) was also studied by DTA–TG in order to compare its evolution as a function of the temperature with respect to the synthesized powders. The residual nitrogen content was determined with a LECO TC-436 nitrogen analyzer, using the gas fusion method. Phase identification was carried out by X-ray diffraction (XRD) using a Siemens D-5000 Diffractometer, operating at 50 kV and 30 mA with a Cu Kα radiation and a Ni filter, in the range $2\theta = 10$–$80°$. The step size was 0.05° and the counting time 1.5 s. The agglomerate size distribution was obtained using a laser analyzer (Malvern Instruments, model Mastersizer). Specific surface area of the calcined powders at 800 °C for 12 h were determined by BET method using N_2 as the adsorbate under high vacuum at 120 °C (Monosorb Surface Area Analyzer MS-13, Quanta Chrome). The frequencies of the absorption bands were analyzed through Fourier transform infrared spectroscopy (Perkin-Elmer FT-IR 1760X) for the as-prepared material and the calcined powders. The pellets used for analysis were made of 0.01 g of the sample powders and 0.3 g of KBr. The powder morphology and composition were studied by scanning electron microscopy coupled to energy dispersive X-ray spectroscopic analysis (SEM–EDS) using a Zeiss DSM 950 microscope and transmission electron microscopy coupled to energy dispersive X-ray spectroscopic analysis (TEM–EDS) using a JEOL JEM 2000 FX microscope. TEM pictures were also used to determine the crystallite size. The shrinkage behavior study was performed using a high temperature dilatometer (Adamel Lhomargy, DI-24 model) at a heating rate of 2°/min up to 1500 °C, on uniaxially and isostatically pressed (200 MPa) discs 2–3 mm thick and 6 mm in diameter. Sintering process was carried out in a furnace in air at 1200 °C for 4 h. The density of the sintered samples was measured through the Arquimedes method, using a Mettler H10 balance. The sintered sample surfaces were polished with diamond powders (6, 3 and 1 μm), thermally etched and analyzed by SEM–EDS. The stability test of the sintered samples was examined in a sealed cell, similar to an autoclave, constructed of a teflon inner casing and stainless steel outer casing (cell volume ≈ 20 cm^3). Sintered pellets were deposited in the cell with 2 ml of deionized water before sealing and heated in an oven from 120 to 170 °C. The longest experiment lasted 48 h.

3. Results and discussion

Fig. 1 shows the DTA–TG data of the as-prepared $La_{0.9}Sr_{0.1}PO_4$ powder and of the NH_4NO_3 commercial powder. In the first case, a 20% weight loss is observed before

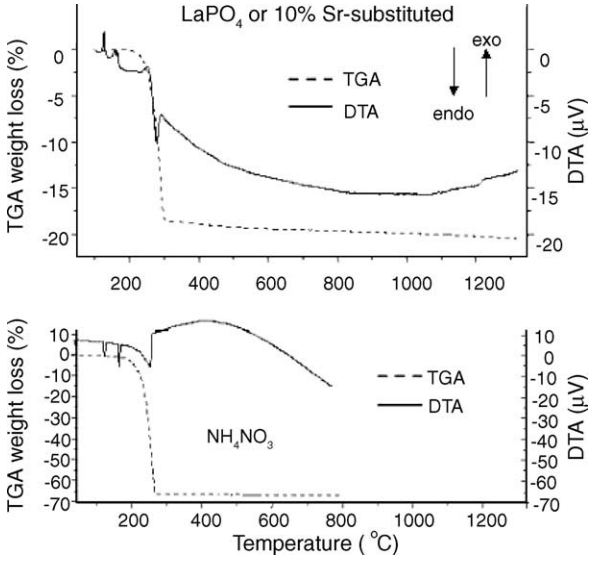

Fig. 1. Simultaneous DTA–TG curves of the as-prepared powders ($LaPO_4$ and $x = 0.10$) and NH_4NO_3 commercial powder, respectively.

250 °C, in the same temperature range three endothermic peaks are observed in the DTA curve. The second set of data, corresponding to NH_4NO_3, is shown to outline that the endothermic peaks of the coprecipitation product data can be due to the presence of this nitrate, a byproduct of the reaction. In fact, the DTA peaks detected in both sets of data can be explained as the transition phase, melting and decomposition of NH_4NO_3,[6] respectively. In contrast, the weight loss that is observed in the TGA curve can be due to the loss of water retained in the inner parts of the phosphate and to the decomposition of NH_4NO_3. The Nitrogen content analysis of the powders confirms the presence of this element in the as-prepared powders. The residual N_2 weight percentage in the as-prepared powders is equal to 10.0 wt.% for all the compositions. This percentage decreases to 3.0 wt.% after the calcination at 200 °C for 12 h and 1.5 wt.% after the calcination at 400 °C for 12 h. After calcination at 800 °C for 12 h, the nitrogen content is less than the experimental error. Similar results are obtained for all compositions. $LaPO_4$ as-prepared powder was washed using absolute ethanol in order to eliminate NH_4NO_3 before calcination. The percentage of N_2 in this case was reduced to 1.5 wt.% after drying at 100 °C. Washing with ethanol therefore reduces the Nitrogen content from 10.0 to 1.5 wt.%. However, the Sr-doped $LaPO_4$ as-prepared powders should not be washed with absolute ethanol due to the loss of Sr^{2+} ions, as was confirmed by ICP-AES analysis.

The agglomerate size distribution for the as-prepared powders is bimodal and shows a size range between 0.1 and 100 μm. The maxima of this distribution occur at 0.4 and 20 μm. The distribution range for the calcined powders is the same (0.1–100 μm) but the position of the second maximum changes to 40 μm after calcination at 200 °C and to 90 μm after calcination at 800 °C. It indicates the expected increase of the agglomerate size due to the calcination treatment. This does not seem to be a problem for the densification process because the agglomerates can be easily reduced through an attrition-milling step applied after the calcination process. The BET specific surface area of the calcined and attrition-milled powders was determined to be around 57 m^2/g in both the undoped and doped samples.

Fig. 2 shows the XRD data of the as-prepared and dried $LaPO_4$ powders and the same powders after different calcination treatments (at 200, 400 and 800 °C). The powder is already crystalline before the calcination and the peak positions correspond to monazite-type $LaPO_4$ (PDF 32-0493). The intensity of the peaks increases very slightly with the calcination temperature and, at the same time, the full width at half maximum (FWHM) decreases. For the Sr-substituted $LaPO_4$ powders, the d-spacings of the doped powders are not shifted with respect to the pure-$LaPO_4$. This fact is quite an important information from the electrical point of view and might indicate that Sr^{2+} ions substitute La^{3+} ions into the $LaPO_4$ monoclinic crystal. This is not unexpected because the ionic radii of both cations are quite similar.[7]

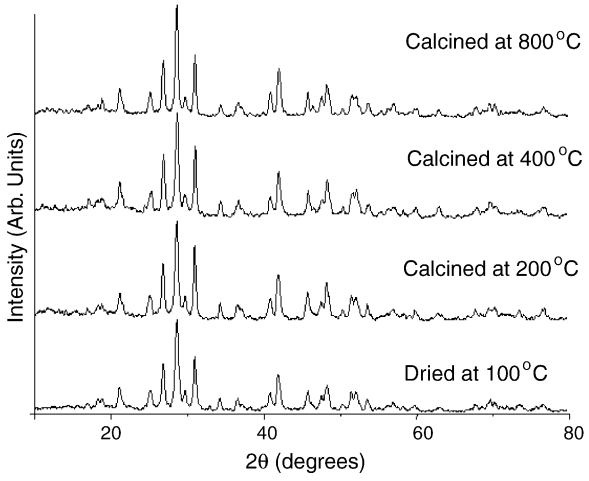

Fig. 2. XRD patterns of the as-prepared $LaPO_4$ powder.

The infra-red spectra of $LaPO_4$ at different temperatures can be observed in Fig. 3. The data present the characteristic bands of the rare earth phosphate (assigned to the PO_4^{3-} group) in the 500–1100 cm^{-1} wavenumber range[8] for both the calcined and uncalcined powders. The wavenumbers are: 1093, 1060, 1024, 993, 954, 617, 579, 564 and 541 cm^{-1}. The bands observed at 3500 and 1620 cm^{-1} can be attributed to the presence of water (stretching vibration of the O–H bond) adsorbed by KBr during the preparation of pellets and to the residual water in the prepared powders. The band observed at 3100 cm^{-1} may be due to the stretching vibrations of O–H and N–H associated bonds. This band is not present in the powders calcined at 400 °C and higher temperatures. The extra-band located at 1380 cm^{-1} is attributed to N–O bond in NO_3^-. This band is eliminated through a calcination at 800 °C/12 h. The spectra of the Sr-substituted powders show the same characteristics.

The micrographs of the powders obtained through SEM (Fig. 4) indicate that the presence of agglomerates with size between 0.1 and 100 μm, as was determined by the laser diffraction analysis. After the calcination, the number of larger agglomerates increases (40 μm at 200 and 400 °C and

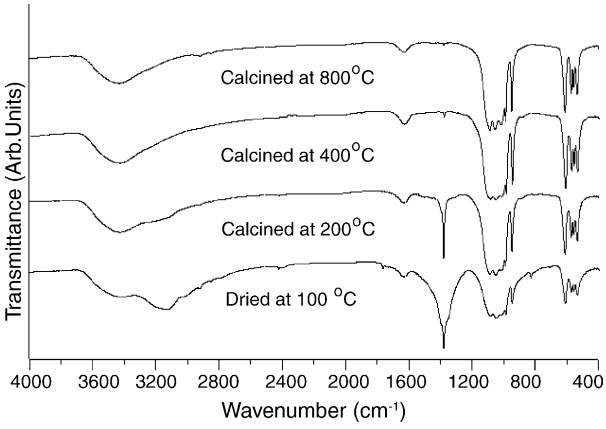

Fig. 3. Infrared spectra of $LaPO_4$ powder.

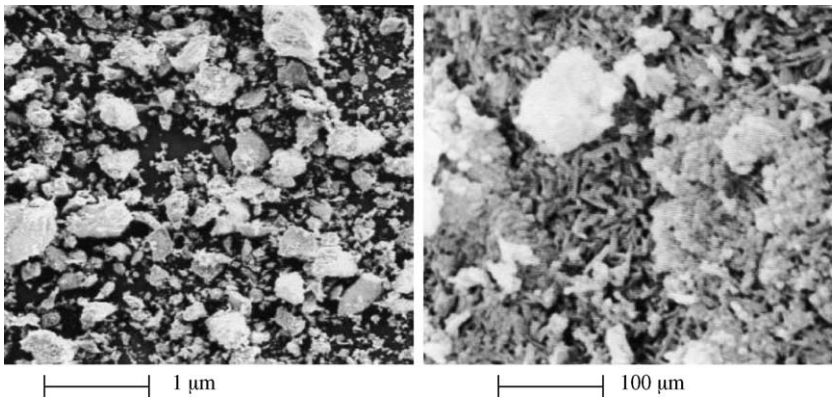

Fig. 4. SEM micrograph at two different magnifications of $LaPO_4$ powders calcined at 400 °C for 12 h.

90 μm at 800 °C). The substitution of La by Sr does not affect the morphology of the powder.

Transmission electron micrographs of the as-prepared powders (Fig. 5a) show individual crystals with needle shape, characteristic of the rhabdophane-type $LaPO_4$ phase, and size between 5 and 50 nm. However, XRD indicates that the dried powder corresponds to the monazite-type phase. We think that the hydration of the dried powder during the preparation of the sample produces the transformation of the monazite to rhabdophane phase. Typically, agglomerates of very fine crystals produce the electron diffraction rings shown in Fig. 5a, indicating that they are polycrystalline powders. If the powder is calcined, a change in the morphology is observed (Fig. 5b). When the powder is calcined at 800 °C for 12 h, the spherical particles have a size between 20 and 50 nm. In the inset in Fig. 5b, a selected area electron diffraction pattern of a $LaPO_4$ crystal showing good crystallinity is presented.

For undoped samples densification is complete at 1200 °C; however for strontium-doped pellets, densification is complete at lower temperatures (≈1100 °C for $x = 0.10$). Thus, the presence of Sr enhances the densification process. In all cases, the density of the sintered samples is higher than 99% of the theoretical density.

Finally, Fig. 6 shows a typical microstructure of a $La_{0.975}Sr_{0.025}PO_4$ sample sintered at 1200 °C for 4 h, after polishing and thermal etching. Fully densified bodies were obtained at this temperature. Second phases were not detected. Nevertheless, an abnormal grain growth is observed, it might be due to inhomogeneity in the green compacts. This might be related to the bimodal agglomerate size distribution observed in both the as-prepared and calcined powders.

The stability of samples in water was examined by exposing sintered pellets for a period of 48 h in the reaction vessel within a temperature range of 120–170 °C, corresponding to a pH_2O range of 2.7–11.5 atm according

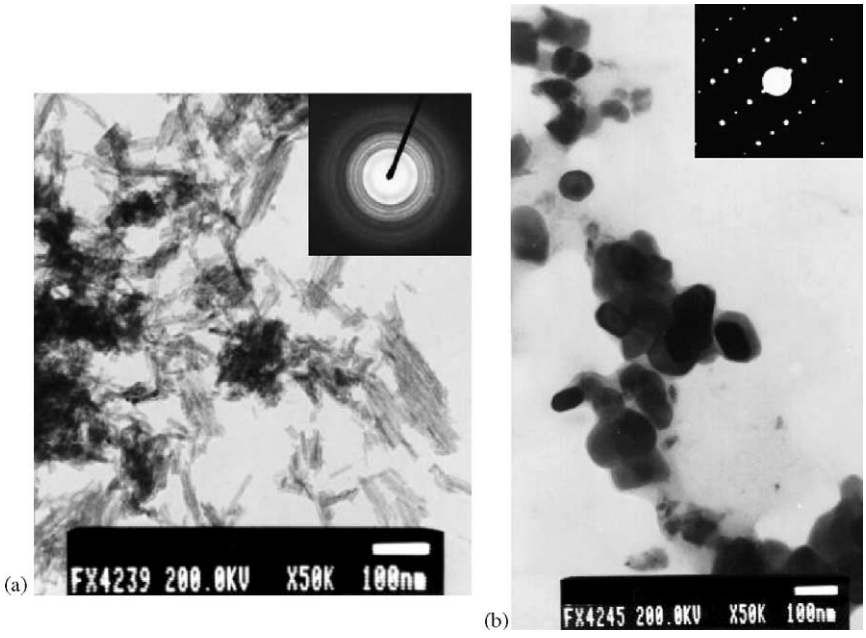

Fig. 5. TEM micrograph of $LaPO_4$ as-prepared (a) and calcined at 800 °C/12 h (b) powder.

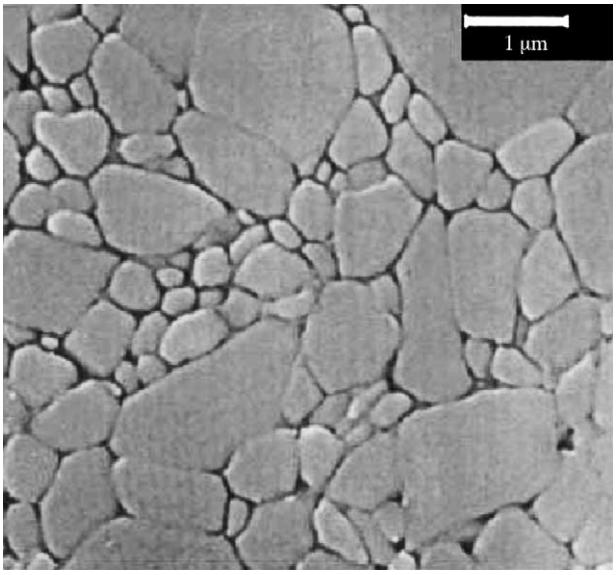

Fig. 6. SEM micrograph of $La_{0.975}Sr_{0.025}PO_4$, sintered at 1200 °C and 4 h, after polishing and thermal etching.

to the Clausius–Clapeyron equation. The cell environment contains a mixture of superheated water and a water–vapor partial pressure that is much higher that would be feasible in a high temperature fuel cell based on a proton-conducting electrolyte. Under these conditions the samples are stable, as observed by XRD, weight measurements and SEM–EDS. The high stability of these materials is a key factor for the application of Sr:$LaPO_4$ as electrolyte in high temperature fuel cells based on protonic conductors.

4. Conclusions

The coprecipitation method was used to obtain nanocrystalline $La_{(1-x)}Sr_xPO_4$ (from 5 to 50 nm) powders at room temperature. NH_4NO_3 is obtained as a byproduct of the coprecipitation reaction. According to the nitrogen analysis, the nitrate is totally eliminated after calcination at 800 °C. The XRD data indicate that the peaks position do not change with the subtitution of La^{3+} by Sr^{2+} into the monazite-type $LaPO_4$ lattice. In addition, as the size of the two ions is quite similar, it is possible that the Sr^{2+} ions occupy the La^{3+} position in the monazite-type $LaPO_4$ crystal. The presence of Sr enhances the densification process in the green compacts. No second phases are observed in the sintered materials. The stability tests of the sintered samples indicate that this material is stable under a pH_2O of 11.5 atm and temperatures up to 170 °C; this characteristic makes $LaPO_4$ a candidate material as electrolyte for SOFC.

Acknowledgments

The authors wish to thank the RTN Network Program High Temperature Proton Conductors (HiTP). “Investigation of high temperature solid proton conductors of relevance to fuel processing and energy conversion applications” (HPRN-CT-2000-00042).

References

1. Norby, T. and Christiansen, N., Proton conduction in Ca- and Sr-substituted $LaPO_4$. *Solid State Ionics*, 1995, **77**, 240–243.
2. Norby, T., Solid-state protonic conductors: principles, properties, progress and prospects. *Solid State Ionics*, 1999, **125**, 1–11.
3. Iwahara, H., Technological challenges in the application of proton conducting ceramics. *Solid State Ionics*, 1995, **77**, 289–298.
4. Tyholdt, F., Horst, J. A., Jørgensen, S., Østvold, T. and Norby, T., Segregation of Sr in Sr-doped $LaPO_4$ ceramics. *Surf. Interface Anal.*, 2000, **30**, 95–97.
5. Gallini, S., Hänsel, M., Norby, T., Colomer, M. T. and Jurado, J. R., Impedance spectroscopy and proton transport number measurements on Sr-substituted $LaPO_4$ prepared by combustion synthesis. *Solid State Ionics*, 2003, **162-163**, 167–173.
6. Mackanzie, R. C., *Differential Thermal Analysis* (*Vol 1*). Academic Press, 1970, p. 345.
7. Montel, J.-M., Devidal, J.-L. and Avignant, D., X-ray diffraction study of brabantite–monazite solid solutions. *Chem. Geol.*, 2002, **191**, 89–104.
8. Farmer, V. C., In *The Infrared Spectra of Minerals*, ed. V. C. Farmer. Mineralogic Society, London, 1974.